Thrombosis Journal

RESEARCH

Open Access

SERPINC1 c.1247dupC: a novel *SERPINC1* gene mutation associated with familial thrombosis results in a secretion defect and quantitative antithrombin deficiency

Maximilian Ruf[1], Sarah Cunningham[1], Alexandra Wandersee[1], Regine Brox[1], Susanne Achenbach[1], Julian Strobel[1], Holger Hackstein[1] and Sabine Schneider[1*]

Abstract

Background Antithrombin (AT) is an important anticoagulant in hemostasis. We describe here the characterization of a novel AT mutation associated with clinically relevant thrombosis. A pair of sisters with confirmed type I AT protein deficiency was genetically analyzed on suspicion of an inherited *SERPINC1* mutation. A frameshift mutation, c.1247dupC, was identified and the effect of this mutation was examined on the cellular and molecular level.

Methods Plasmids for the expression of wild-type (WT) and mutated *SERPINC1* coding sequence (CDS) fused to green fluorescent protein (*GFP*) or hemagglutinin (*HA*) tag were transfected into HEK293T cells. Subcellular localization and secretion of the respective fusion proteins were analyzed by confocal laser scanning microscopy and Western blot.

Results The c.1247dupC mutation results in a frameshift in the CDS of the *SERPINC1* gene and a subsequently altered amino acid sequence (p.Ser417LysfsTer48). This alteration affects the C-terminus of the AT antigen and results in impaired secretion as confirmed by GFP- and HA-tagged mutant AT analyzed in HEK293T cells.

Conclusion The p.Ser417LysfsTer48 mutation leads to impaired secretion, thus resulting in a quantitative AT deficiency. This is in line with the type I AT deficiency observed in the patients.

Keywords Hereditary antithrombin deficiency, Frameshift mutation, Secretion defect, Thrombosis

Background

AT is a single-chain glycoprotein (464 amino acids containing a 32 amino acid N-terminal signal peptide) and is secreted as a 432 amino acid protein by hepatocytes into the blood stream [1, 2]. AT has two major binding sites for interaction partners: the heparin-binding site at the N-terminus and the reactive site at the C-terminus. AT acts as a serine protease inhibitor (SERPIN) by binding covalently with the Arg425-Ser426 peptide bond in its reactive center loop to the active site of serine proteases in the blood. This way AT inactivates, next to other serine proteases, coagulation factors IIa (thrombin), IXa, Xa, XIa and XIIa [1, 2].

There are two types of AT deficiencies. Type I deficiency is characterized by concordant reduction of protein level and activity, while type II deficiency is defined by normal protein levels but a reduced functionality.

*Correspondence:
Sabine Schneider
sabine.schneider@uk-erlangen.de
[1] Department of Transfusion Medicine and Hemostaseology, Friedrich-Alexander-University Erlangen-Nürnberg (FAU), University Hospital Erlangen, Krankenhausstr. 12, 91054 Erlangen, Germany

Type II deficiency of AT can be subdivided into three groups depending on the affected domain of the AT protein. In type IIa, mutations affect the reactive site, in type IIb, mutations affect the heparin-binding site and in type IIc, mutations show different defects in other parts of the protein [3]. Independent of its classification, AT deficiency, with a prevalence of 0.1–0.3% within the Caucasian population, poses a major risk for thromboembolic events [4, 5].

Methods

Samples

The here discussed patients were two sisters who were diagnosed with AT deficiency after multiple thromboembolic events. Patient 1, a 64-year-old woman, suffered from a bilateral deep vein thrombosis (DVT) as a teenager with recurrence after a temporary change in her anticoagulation treatment from phenprocoumon to acetylsalicylic acid. The treatment regimen was switched back to phenprocoumon after the DVT. Her sister (patient 2), a 65-year-old woman, had multiple DVT events in her right lower leg and pulmonary embolism as a teenager. The patient also developed a DVT in her right leg at the age of 27 during pregnancy eight weeks before delivery. The intake of an oral contraceptive during the time of their first thrombotic events was postulated as a possible triggering factor. In addition, both patients have been diagnosed with a heterozygous factor V Leiden (FVL) mutation. According to the family history, the patients´ father was diagnosed with AT deficiency. No statement could be made from the patients as to whether their parents suffered from thromboembolic events. Additionally, the patients could not provide any information regarding the heredity of the FVL mutation within their family.

Blood samples from healthy blood donors of the blood donation center of the Clinical Department of Transfusion Medicine and Hemostaseology in Erlangen served as control material within the study. The study was conducted in accordance with the Declaration of Helsinki, and approved by the Ethics Committee of the Friedrich-Alexander-University Erlangen-Nürnberg (FAU) (#477_20 B, #357_19 B, #343_18 B). Written informed consent was obtained from all participants of the study.

Determination of AT parameters

AT activity and AT antigen levels were analyzed with a STA Max instrument (Diagnostica Stago S.A.S., Asnières-sur-Seine, France), using the STACHROM AT III Kit for activity and the LIATEST AT III kit for antigen levels (Diagnostica Stago S.A.S., Asnières-sur-Seine, France).

DNA isolation

Genomic DNA was automatically isolated from whole blood and quantified using commercial kits (NucleoSpin® 8 Blood Core Kit, Macherey Nagel, Düren, Germany for isolation, QuantiFluor® dsDNA System, Promega, Madison, WI, USA for quantification) and a Hamilton Microlab Starlet robot (Reno, NV, USA) and microplate fluorometer (Berthold, Bad Wildbad, Germany).

Next generation sequencing

The CDS (according to transcript NM_000488.3) and adjacent intron regions of the *SERPINC1* gene were sequenced with an Illumina amplicon-based gene panel (AmpliSeq™ Custom DNA Panel for Illumina®) on a MiSeq machine (Illumina®, San Diego, CA, USA) in accordance to the manufacturer's instructions. The custom DNA panel enabled CDS and adjacent intron regions sequencing of the following genes: *F7*, *F9*, *F13A1*, *F13B*, *F11*, *FGA*, *FGB*, *FGG*, *PROC*, *PROS1*, *SERPINC1* and *VWF* [6].

Next generation sequencing data was thereafter analyzed with the SeqNext Software version 5.2.0 (JSI Medical Systems, Ettenheim, Germany).

Database submission

The c.1274dupC frameshift mutation was submitted to ClinVar (www.ncbi.nlm.nih.gov/clinvar; accession SCV002520629).

Quantitative mutation screening

To gage the prevalence of the c.1247dupC frameshift mutation within the general population, 358 healthy individuals were screened with a sequence-specific primer polymerase chain reaction (SSP-PCR) as described before [6]. Oligonucleotides were obtained from Merck (Darmstadt, Germany). Primer combinations consisted of the following: SERPINC1g+13006f (5'-AGTACCTTACATTCTCTGCATGA-3') and SERPINC1g+13243r-WT (5'-CAATCACAACAGCGGTACTTGC-3') for the *SERPINC1* WT allele (resulting in a 238 bp fragment) and SERPINC1g+13006f and SERPINC1g+13243r-SNP (5'-CAATCACAACAGCGGTACTTGG-3') for detecting the *SERPINC1* c.1247dupC frameshift mutation (resulting in a 239 bp fragment). The co-amplification of the human growth hormone gene (*GH1*) with primers GH1g+334f (5'-TGCCTTCCCAACCATTCCCTTA-3') and GH1g+768r (5'-CCACTCACGGATTTCTGTTGTGTTTC-3'), resulting in a 434 bp fragment, served as an internal control.

Construct generation

Plasmids for HEK293T cell transfection were created using Gibson Assembly [7], according to the manufacturer's instruction manual (Gibson Assembly® Master Mix/Gibson Assembly® Cloning Kit NEB, New England Biolabs, Ipswich, MA, USA). Oligonucleotides for Gibson Assembly were designed using NEBuilder Assembly Tool (https://nebuilder.neb.com/#!/) and were manufactured by Merck (Darmstadt, Germany). Vector pcDNA3.1(+)/Puro/FA/GFP-LL5BIP [kindly provided from Tomasz Prószyński (Addgene plasmid # 112829; http://n2t.net/addgene:112829; RRID:Addgene_112829)] was used for the expression of the *GFP* fusion. For plasmid pMR01 (*SERPINC1-GFP*) insert sequences and vector fragments with complementary overhangs were amplified by PCR using primers (and templates) as follows:

- *SERPINC1* CDS fragment: MR01-SERPINC1_fwd (5'-GTACCGAGCTCGGATCCATGTATTCCAATGTGATAGGAACTGTAACCTCTG-3'), MR01-SERPINC1_rev (5'-CACCATACCGCTACCGCCGCCGCTGCCACCCTTAACACAAGGGTTGGCTACTCTGC-3') (human antithrombin III cDNA ORF Clone, obtained from SinoBiological, Beijing, China)
- GFP CDS fragment: MR01-GFP_fwd (5'-GTTAAGGGTGGCAGCGGCGGCGGTAGCGGTATGGTGAGCAAGGGCGAGGAG-3'), MR01-GFP_rev (5'-GCACAGTCGAGGCTGATCACTTGTACAGCTCGTCCATGCCG-3') (pcDNA3.1(+)/Puro/FA/GFP-LL5BIP)
- vector pcDNA3.1 backbone: pcDNA3.1_fwd (5'-GGACGAGCTGTACAAGTGATCAGCCTCGACTGTGCCTTCTAG-3'), pcDNA3.1_rev (5'-CTATCACATTGGAATACATGGATCCGAGCTCGGTACCAAG-3' (pcDNA3.1(+)/Puro/FA/GFP-LL5BIP).

For plasmid pMR02 (*SERPINC1*$_{c.1247dupC}$-GFP) the c.1247dupC mutation was introduced by site-directed mutagenesis using the Q5 Site-Directed Mutagenesis Kit (New England Biolabs, Ipswich, MA, USA) [8], with the primer combination M1-pBWCS2_DupC_fwd (5'-GCAGCTGCCAAGTACCGCTGTTGTG-3') and M1-pBWCS2_DupC_rev (5'-CGGTACTTGGCAGCTGCTTCACTG-3'). To deal with the resulting frameshift that also affects the CDS of *GFP*, *SERPINC1* c.1247dupC CDS was amplified with oligonucleotides MR01-SERPINC1_fwd (5'-GTACCGAGCTCGGATCCATGTATTCCAATGTGATAGGAACTGTAACCTCTG-3') and MR02-ohne Stop_rev (5'-GCTACCGCCGCCGCTGCCACCACACAAGGGTTGGCTACTCTGCC-3') followed by the assembly into the pMR01 backbone (obtained with primer combination MR02-GGSG-EGFP_fwd: 5'-GGTGGCAGCGGCGG-3' and MR01-pcDNA3.1_rev: 5'-CTATCACATTGGAATACATGGATCCGAGCTCGGTACCAAG-3'). During the PCR amplification for the Gibson Assembly a 2×GGSG linker was introduced in front of the GFP in both pMR01 and pMR02.

The HA tag fusion vector was generated by digesting pcDNA3.1(+)/Puro/FA/GFP-LL5BIP with HindIII and XbaI to remove the GFP-LL5BIP cassette. Oligonucleotides encoding a 2×GGSG linker and a 3×HA tag (HindIII-GGSG-3xHA-Tag-XbaI_fwd: 5'-CTAGATCAAGCATAGTCAGGTACGTCATAAGGGTAAGATCCAGCATAGTCAGGTACGTCATAAGGGTAAGATCCAGCATAGTCAGGTACGTCATAAGGGTAACCGCTACCGCCA-3' and HindIII-GGSG-3xHA-Tag-XbaI_rev: 5'-CTAGATCAAGCATAGTCAGGTACGTCATAAGGGTAAGATCCAGCATAGTCAGGTACGTCATAAGGGTAAGATCCAGCATAGTCAGGTACGTCATAAGGGTAACCGCTACCGCCA-3') were annealed, leading to a double-stranded DNA fragment with HindIII and XbaI overhangs. This fragment was ligated into the HindIII/XbaI digested pcDNA3.1 backbone, resulting in the HA tag expression vector pBWCS3.

Insert and vector fragments for plasmid pMR03 (*SERPINC1-HA*) were amplified using primers (and template) as follows:

- *SERPINC1* CDS fragment: MR03_SERPINC-3xHA_fwd (5'- GCTAGCGTTTAAACTTAAGCTTATGTATTCCAATGTGATAGGAACTGTAACCTCTG-3'), pMR03_rev (5'-CATAAGGGTAACCGCTACCGCCGCCGCTGCCACCCTTAACACAAGGGTTGGCTACTCTGC-3') (pMR01)
- vector pBWCS3 backbone: pBWCS3-GGSG-3xHA_fwd (5'-GGCGGTAGCGGTTACCCTTATG-3'), pBWCS3-GGSG-3xHA_rev (5'-AAGCTTAAGTTTAAACGCTAGCCAGCTTG-3') (pBWCS3).

For plasmid pMR04 (*SERPINC1*$_{c.1247dupC}$-HA) the insert and vector fragments were amplified by PCR using the following primers (and template):

- *SERPINC1* c.1247dupC: MR03_SERPINC-3xHA_fwd (5'-GCTAGCGTTTAAACTTAAGCTTATGTATTCCAATGTGATAGGAACTGTAACCTCTG-3'), pMR04_rev (5'-CATAAGGGTAACCGCTACCGCCGCCGCTGCC ACCACACAAGGGTTGGCTACTCTGC-3') (pMR02)
- vector pBWCS3 backbone: pBWCS3-GGSG-3xHA_fwd (5'-GGCGGTAGCGGTTACCCTTATG-3'), pBWCS3-GGSG-3xHA_rev (5'-AAGCTTAAGTTTAAACGCTAGCCAGCTTG-3') (pBWCS3).

Plasmid sequences were validated and confirmed by Sanger sequencing (Eurofins Genomics Germany GmbH, Ebersberg, Germany).

HEK293T clone generation

HEK293T cells (ACC 635, DSMZ, Braunschweig, Germany) were grown in DMEM (#D6429, Sigma-Aldrich, Taufkirchen, Germany) supplemented with 10% FCS (anprotec, Bruckberg, Germany), 1% GlutaMAX (Thermo Fisher Scientific, Waltham, MA, USA), 1% Penicillin–Streptomycin (Sigma-Aldrich, Taufkirchen, Germany) at 37°C and 5% CO_2 in a humidified incubator. Cells were transfected with *Trans*IT®-293 Reagent (Mirus Bio LLC, Madison, WI, USA) following the manufacturer´s recommendations. After 24 h the medium was replaced with fresh medium containing 5 µg/ml Puromycin (Carl Roth, Karlsruhe) to select the transfected cells. Clones were picked after 1–2 weeks and analyzed for the presence of the respective tag by flow cytometry (CytoFLEX S, Beckman Coulter, Brea, CA, USA). HEK293T cells transfected with pMR01 and pMR02 were analyzed for direct *GFP* expression while *HA*-tag expression of HEK293T cells transfected with pMR03 and pMR04 was assessed by intracellular staining in accordance to the manufacturer's protocol (HA Tag Monoclonal antibody Dy550, #26183D550, Life Technologies, Carlsbad, CA, USA; eBioscience™ FOXP3-staining kit, #00–5523-00, Thermo Fisher Scientific, Waltham, MA, USA). Up to six cell lines were picked for each plasmid transfection and used for subsequent confocal laser scanning microscopy and Western blot.

Prior to microscopic analysis, HEK293T cells expressing plasmid pMR01 or pMR02 were transfected prior to imaging with the ER-Tracker™ Red (glibenclamide BODIPY® TR) (Thermo Fisher Scientific, Waltham, MA, USA) for 30 min following the manufacturer´s recommendations.

Confocal laser scanning microscopy

A Leica TCS SP8 confocal laser scanning microscope (Leica, Wetzlar, Germany) was used for imaging with 488 nm (GFP) and 552 nm (RFP) laser light for excitation. GFP fluorescence was detected in a window ranging from 495–520 nm and RFP fluorescence in a window ranging from 570–595 nm. Data processing was performed with the Leica Application Suite X software version 2.0.1.14392 (Leica, Wetzlar, Germany).

Western blotting

In order to quantify protein content and secretion, respective HEK293T clones were cultured at 2×10^6–1×10^7 cells/ml in serum-free culture medium (#14571C, EX-CELL®, Merck, Darmstadt, Germany) without antibiotics for 48 h. Cells were subsequently harvested by resuspension and centrifuged at 300 g for 5 min. Supernatants were collected, mixed with the cOmplete™ Mini protease inhibitor-cocktail (Merck, Darmstadt, Germany) and subsequently stored at -20°C. The cell pellets were lysed with Radioimmunoprecipitation Assays buffer (RIPA: 50 mM Tris–HCl, pH 8.0, 150 mM NaCl, 0.5% sodium deoxycholate, 0.1% Triton X-100 and 0.1% SDS) and the cOmplete™ Mini protease inhibitor-cocktail (Merck, Darmstadt, Germany) for 30 min on ice. Samples were subsequently centrifuged at 11,000 g for 10 min at 4°C. The ensuing cell lysate supernatants were transferred into a fresh tube and stored at -20°C until further use.

Protein concentrations were determined with a Bradford assay (Roti®-Nanoquant #K880.1, Carl Roth, Karlsruhe, Germany) according to the manufacturer's protocol. The measurement was performed on a Fluostar Omega (BMG Labtech, Ortenberg, Germany) at 590/450 nm.

SDS-PAGE was performed with 40 µg protein from cell lysates and 5 µg protein from supernatant reduced in 4×Laemmli-buffer (Roti®-Load1, #K929.1, Carl Roth, Karlsruhe, Germany). Samples were denaturized at 95°C for 5 min and subsequently loaded onto 4–15% Mini-PROTEAN® TGX™ Precast Protein Gels (Bio-Rad, Hercules, CA, USA). Protein bands were seperated at 100 V for 1 h with Western Blot Running Buffer (25 mM TRIS Base, 192 mM Glycin, 0.1% SDS; pH 8.3) using the Mini-PROTEAN® Tetra Vertical Electrophoresis System (Bio-Rad, Hercules, CA, USA). After separation, gels were blotted onto a nitrocellulose membrane (#GE10600003, Amersham™ Protran® Premium, Sigma-Aldrich, Taufkirchen, Germany) at 100 V for 1 h (Mini Trans-Blot Module, Bio-Rad, Hercules, CA, USA).

Membranes were washed in Tris-buffered saline with Tween solution (TBST: 20 mM TRIS, pH 7.5, 150 mM NaCl, 0.1% Tween-20) and blocked with TBST containing 5% milk powder (Carl Roth, Karlsruhe, Germany) for 1 h at room temperature. Immunostaining of GFP fusion proteins of cell lysate and supernatant samples was done with GFP Polyclonal Antibody, DyLight™ 800 (1:10,000 dilution; #600–145-215, Thermo Fisher Scientific, Waltham, MA, USA). HA tagged proteins within cell lysate and supernatant samples were immunostained with HA Tag Monoclonal Antibody (2–2.2.14), DyLight™ 550 (1:1000 dilution; #26183D550, Thermo Fisher Scientific, Waltham, MA, USA). GAPDH Loading Control Monoclonal Antibody (GA1R), DyLight™ 680, Thermo Fisher Scientific, Waltham, MA, USA, was used to normalize the Western blot. The blots were stained at 4°C overnight and washed the next day three times for 10 min

in TBST. A ChemiDoc Imaging System, Bio-Rad (Hercules, CA, USA) was used for imaging.

GAPDH loading control monoclonal antibody was used for normalization of protein amount from cell lysates. Supernatants were normalized to the total protein content within the stain-free gels. A ChemiDoc MP Imaging System (Bio-Rad, Hercules, CA, USA) was used for imaging.

Statistical analysis

Basic statistics (mean values and standard deviations) were performed using Microsoft Excel 2016 (Office Professional Plus 2016; Microsoft, Redmond, WA, USA) and visualized using GraphPad Prism (version 9.51). Results are shown as mean values ± standard deviation. One-way ANOVA followed by Bonferroni and Holm multiple comparison (all pairs simultaneously compared) (https://astatsa.com/) was used to test for differences between cell lines.

In silico prediction of protein structure

Tertiary structure of WT and mutated AT was predicted using Contact-guided Iterative Threading ASSEmbly Refinement (C-I-TASSER) [9]. Furthermore, iCn3D was used to display the calculated models [10, 11].

Results

Identification of *SERPINC1* mutation c.1247dupC (p.Ser417LysfsTer48)

Patient 1 presented reduced AT antigen levels and reduced AT activity with 44% and 57%, respectively, with normal ranges from 80–120% for both.

Patient 2 also presented reduced AT antigen level of 48% and a reduced AT activity of 60%.

Since a hereditary AT deficiency was suspected, genetic analysis was performed for both patients. The analysis showed the identical heterozygous insertion (c.1247dupC) within exon 7 (according to gene model NM_000488.3) for both patients. This mutation leads to a frameshift within the AT CDS, resulting in a switch from Ser417 to Lys and altering the subsequent 46 amino acids (p.Ser417LysfsTer48; hereafter indicated as AT_{fs}) (Fig. 1A). Coincidentally, the C-terminus of AT_{fs} differs by only one amino acid in length, although the amino acid sequence is completely different.

Three hundred and fifty-eight healthy individuals were screened for the c.1247dupC mutation via SSP-PCR in order to assess the frequency within the general population. Three individuals tested positive within the healthy cohort using the primer combination to amplify the c.1247dupC allele (exemplarily shown for one individual, H2, in Fig. 1B).

There are two known mutations at nucleotide c.1246 that could possibly be detected by the primer combination used for the SSP-PCR screening (underlined DNA sequences in Fig. 1C): $AT_{Charleville}$ (c.1246G>C; p.Ala416Pro) [13] and $AT_{Cambridge\ II}$ (c.1246G>T; p.Ala416Ser) [12], the latter by binding of the reverse primer with reduced specificity. To clarify the *SERPINC1* variants detected in the respective healthy donors, next generation sequencing was performed, revealing that these three individuals were heterozygous carriers of the point mutation c.1246G>T, described as $AT_{Cambridge\ II}$ [12]. One individual gave consent to be contacted in case of relevant findings and was subsequently screened for AT antigen and activity. Both were in lower, but normal range (AT antigen 89%, AT activity 84%, with normal ranges from 80–120% for both).

Confocal microscope analysis of GFP fusions in HEK293T cells

According to the type I deficiency diagnosed in our two patients, a secretory deficiency seemed likely. HEK293T cells were used as an in vitro expression system to study the secretion and subcellular localization of AT_{fs}-GFP in comparison to AT-GFP. Based on the confocal laser scanning microscope analysis no apparent differences could be detected for the subcellular localization of the GFP fluorescence between *SERPINC1-GFP* or *SERPINC1*$_{c.1247dupC}$*-GFP* expressing cells (Fig. 2A, D). Complete co-localization of AT-GFP and AT_{fs}-GFP with ER-Tracker™ Red (Fig. 2B, C, E and F) indicated that both, AT-GFP and AT_{fs}-GFP, were able to correctly enter the secretory pathway. No obvious differences concerning the structure of the endoplasmic reticulum (ER) were observed, indicating that AT_{fs} is potentially not disturbing the structural integrity of the ER (Fig. 2).

Determination of secretion in HEK293T cells

In order to evaluate if the c.1247dupC mutation results in a secretory deficiency, supernatants and cell lysates of *SERPINC1-GFP* or *SERPINC1*$_{c.1247dupC}$*-GFP* expressing HEK293T cell lines were analyzed (Fig. 3A). Three clones per construct were used for Western blot analysis, with three technical repeats per cell line. No significant difference could be observed between the amount of AT-GFP and AT_{fs}-GFP within the cell lysate (Fig. 3A). Comparison of AT-GFP and AT_{fs}-GFP in the cell culture supernatants showed a clear reduction in secretion of AT_{fs}-GFP with a highly significant difference ($p < 0.01$) between all AT_{fs}-GFP cell lines and each AT-GFP line (Fig. 3B). To exclude a potential impact of the GFP tag (which is comparably large with 239 amino acids) on the secretion of the fusion protein, constructs for fusions of AT and AT_{fs} with an HA tag (31 amino acids) were introduced into HEK293T

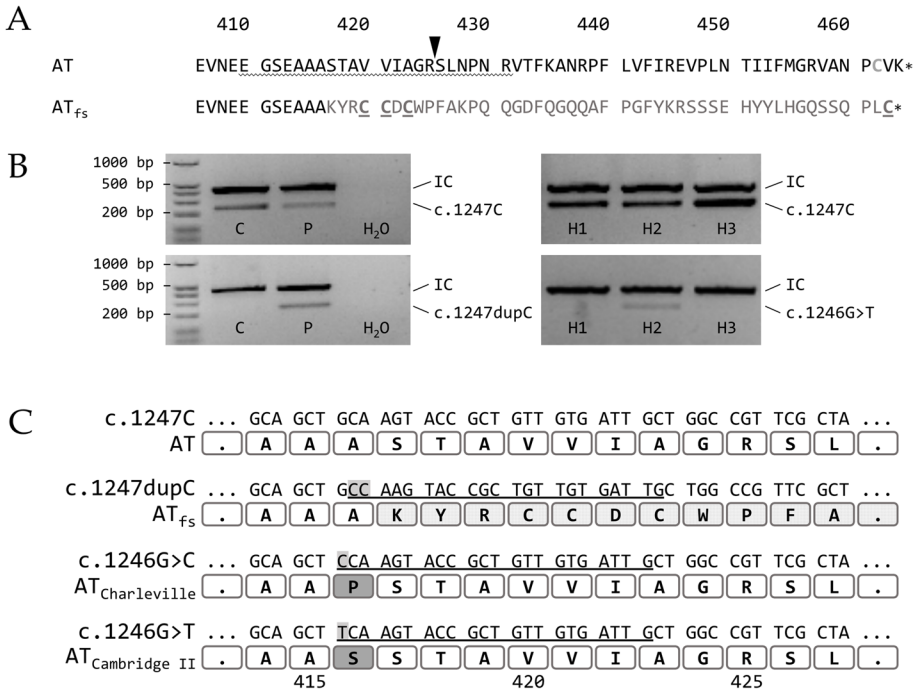

Fig. 1 The *SERPINC1* + 1 frameshift mutation c.1247dupC results in an altered AT C-terminus (p.Ser417LysfsTer48). **A** Comparison of the C-terminal amino acid sequence of WT (AT) and mutant AT (AT$_{fs}$) with amino acid sequence change p.Ser417LysfsTer48 given in gray. The reactive center loop is underlined, the arrowhead indicates the position of the reactive Arg-Ser bond. Cys462, involved in a disulfide bond in AT, is shown in light gray. New Cys residues introduced by the frameshift mutation in AT$_{fs}$ are underlined. **B** Exemplary results of SSP-PCR screening for the *SERPINC1* c.1247dupC mutation in 358 healthy individuals. Upper row: screening for the WT allele using genomic DNA of a healthy individual (C) and a patient described (P) as controls and three out of 358 healthy individuals (H1, H2, H3). The PCR result for the *SERPINC1* WT allele is represented by a 238 bp fragment (c.1247C). Lower row: screening for the c.1247dupC allele. Genomic DNA of a healthy individual (C) and a patient (P) were used as controls. The primer combination for detection of the c.1247dupC allele (239 bp) also amplified the AT$_{Cambridge\ II}$ allele (c.1246G>T) [12], which was found in three out of 358 healthy individuals (H2 shown as example). H$_2$O, water control; IC, internal PCR control (434 bp fragment from *GH1* gene). **C** Comparison of partial DNA sequences of *SERPINC1* WT (c.1247C), the described frameshift mutation (c.1247dupC) and mutations AT$_{Charleville}$ (c.1246G>C) [13] and AT$_{Cambridge\ II}$ (c.1246G>T) [12], which could also possibly be detected. The respectively encoded amino acid sequence is given underneath for orientation. Underlined nucleotides indicate the position of the reverse primer used for detection of the mutant allele; nucleotides highlighted by a gray background indicate the respective mutation. Amino acids highlighted by a dotted background indicate the p.Ser417LysfsTer48 mutation. The Ala416Pro and Ala416Ser exchanges, encoded by the AT$_{Charleville}$ mutation c.1246G>C [13] and AT$_{Cambridge\ II}$ mutation c.1246G>T [12], respectively, are highlighted by a gray background

cells. Western blot analysis was performed analogous to the analysis of GFP-tagged cell lines. Similar results as for the GFP fusions were obtained when analyzing the amount of AT-HA and AT$_{fs}$-HA in cell lysate and cell culture supernatant (Fig. 3C, D). Supernatants of all AT$_{fs}$-HA cells lines presented significantly reduced (p<0.01) secretions of the fusion protein in comparison to each AT-HA line.

These results prove a secretion defect of AT$_{fs}$ which is in accordance with the type I AT deficiency diagnosed in our two patients.

Discussion

We identified the frameshift mutation c.1247dupC in two patients diagnosed with type I AT deficiency. Duplication c.1247dupC results in an AT antigen with a +1 frameshift mutated aberrant C-terminus, p.Ser417LysfsTer48 (AT$_{fs}$). The expression of recombinant constructs in HEK293T cells revealed a clear secretion defect of the AT$_{fs}$ variant. According to literature and database research, mutation p.Ser417LysfsTer48 was so far solely mentioned in one recent publication [14], but neither indicated as a mutation identified in patients nor with an origin given for this mutation. Thus, to the best of our knowledge, we are the first to describe this mutation (i) in patients and (ii) as causative for a diagnosed AT deficiency. The *SERPINC1* c.1247dupC variant could not be identified in 358 healthy probands, thus confirming that it is not a common polymorphism.

However, three of the 358 healthy probands were found to be heterozygous carriers of AT$_{Cambridge\ II}$ (c.1246G>T; p.Ala416Ser) [12]. This mutation has been described to cause transient AT deficiency (i.e., AT parameter can vary between normal and reduced values in different

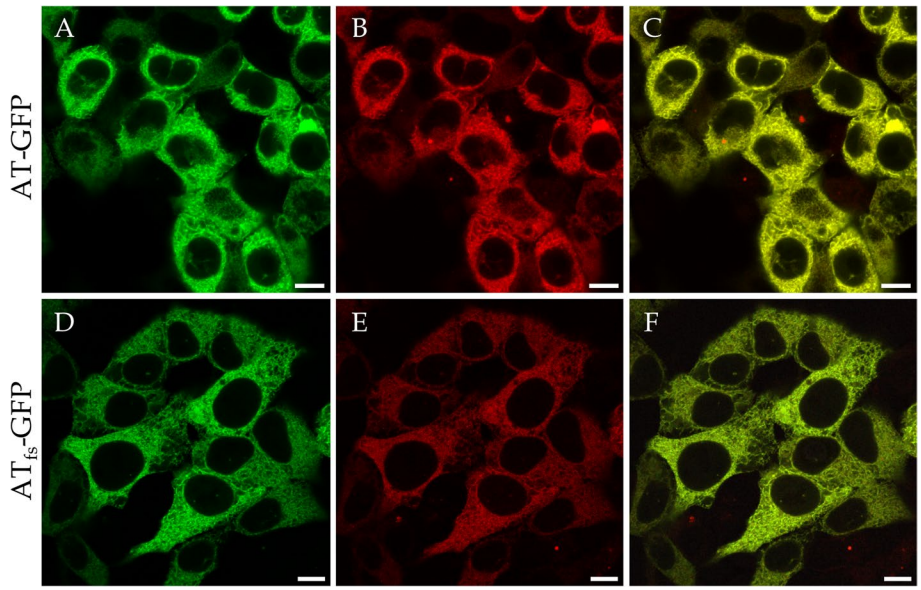

Fig. 2 Subcellular localization of AT-GFP and AT$_{fs}$-GFP in HEK293T cells. HEK293T cells expressing a construct encoding AT-GFP (**A**) or AT$_{fs}$-GFP (**D**) were transfected with ER-Tracker™ Red (**B**, **E**). Both AT-GFP and AT$_{fs}$-GFP were detected within the ER and co-localized with ER-Tracker™ Red (**C**, **F**). GFP fluorescence is shown in green, ER-Tracker™ Red in red and colocalization is indicated in yellow. Scale bars represent 10 µm

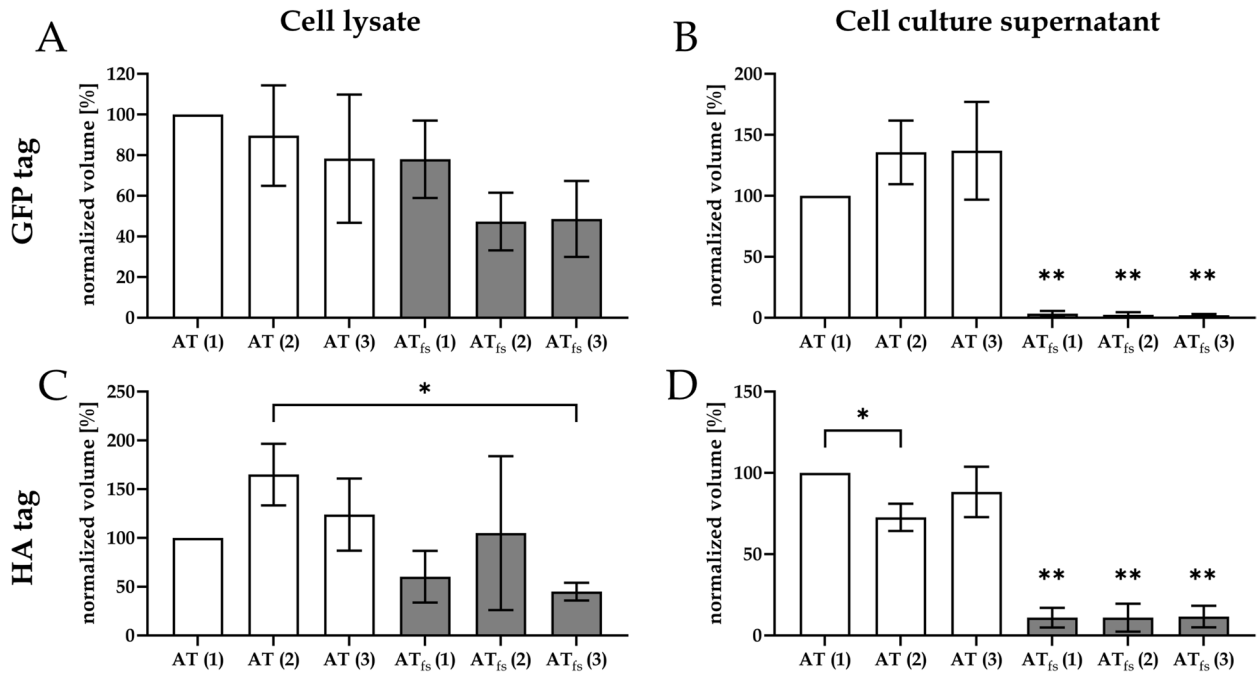

Fig. 3 Frameshift mutation p.Ser417LysfsTer48 results in a secretion defect. Cell lysates and cell culture supernatants of HEK293T cells transfected with constructs for GFP- or HA-tagged AT or AT$_{fs}$ were compared. While no significant quantitative differences could be detected for AT and AT$_{fs}$ in cell lysate between all mutant and all WT lines (**A**, **C**), secretion of AT$_{fs}$ is strongly reduced in all mutant lines compared to all WT lines with a statistical significance of $p<0.01$ (**B**, **D**) (analyzed using one-way ANOVA with Bonferroni and Holm correction, all pairs simultaneously compared). Mean values of $n=3$ technical replicates of three different cell lines per construct, error bars=standard deviation. One asterisk indicates a significant difference ($p<0.05$), two asterisks indicate a highly significant difference ($p<0.01$). If not indicated by brackets, significance refers to all mutant lines compared to all WT lines

measurements for one and the same individual), with pathogenicity depending on environmental factors also [15]. This is in line with AT antigen levels and AT activity in a lower, but normal range und a negative family history for thromboembolic events for the one healthy donor available for further diagnostics. In addition, $AT_{Cambridge\ II}$ has been described to occur with a relatively high prevalence [15, 16]. Thus, although the frequency of $AT_{Cambridge\ II}$ among the analyzed healthy blood donors is surprisingly high, it is still within the realm of possibility.

A recent publication describes several AT mutants with aberrant C-termini due to +1 frameshift mutations [14]. Depending on whether the frameshift mutation occurs (a) upstream or (b) downstream of Phe440, those +1 frameshift AT variants are (a) secreted in a monomeric form or are (b) not secreted, but complexing WT AT into ER aggregates. The latter results in a disturbed ER structure, characterized by fragmentation and dilatation. This dominant-negative effect on WT AT explains, why patients harboring those frameshift variants showed more severely reduced AT activity and AT antigen levels than to be expected from a heterozygous mutation [14].

This phenomenon was not observed for the patients described here. Both had values for AT activity and AT antigen level in accordance with a standard type I AT deficiency, that is, reduction of activity and antigen amount in a range expected for a pathogenic mutation in a heterozygous state (40–60%; [14]). In line with that, secretion of AT_{fs} is strongly impaired (Fig. 3B, D), but the ER structure seems to not differ between HEK293T cells expressing *SERPINC1-GFP* or *SERPINC1*$_{c.1247dupC}$-*GFP* (Fig. 2), as visualized by confocal laser scanning microscopy. Nevertheless, to eventually confirm that the integrity of the ER is in fact not impaired by the AT_{fs} mutation, further analysis by electronic microscopy would be required.

Variations from the native amino acid sequence of AT [17–19] and other SERPINS [20–22] are known to introduce conformational instability, resulting in polymerization by insertion of the reactive center loop of one mutated SERPIN molecule into the β-sheet A of a respective partner SERPIN protein, with a subsequent accumulation leading to serpinopathy [20, 23].

Mutations of a highly conserved Gly residue in strand 5B of AT (Gly456) and other members of the SERPIN family were shown to cause polymerization and intracellular retention, resulting in serpinopathy [19, 23–25]. According to the fact that not only Gly456, but actually 46 amino acids of the AT C-terminus including strands 4B and 5B are affected by the here described p.Ser417LysfsTer48 mutation, polymerization of AT_{fs} as causative for ER retention seems possible.

Interestingly, a computer model generated with C-I-TASSER [9], comparing the (potential) tertiary structure of AT_{fs} to WT AT, shows a still SERPIN-like folding of AT_{fs} comprised of three α-helices and nine β-sheets [26] (Fig. 4B).

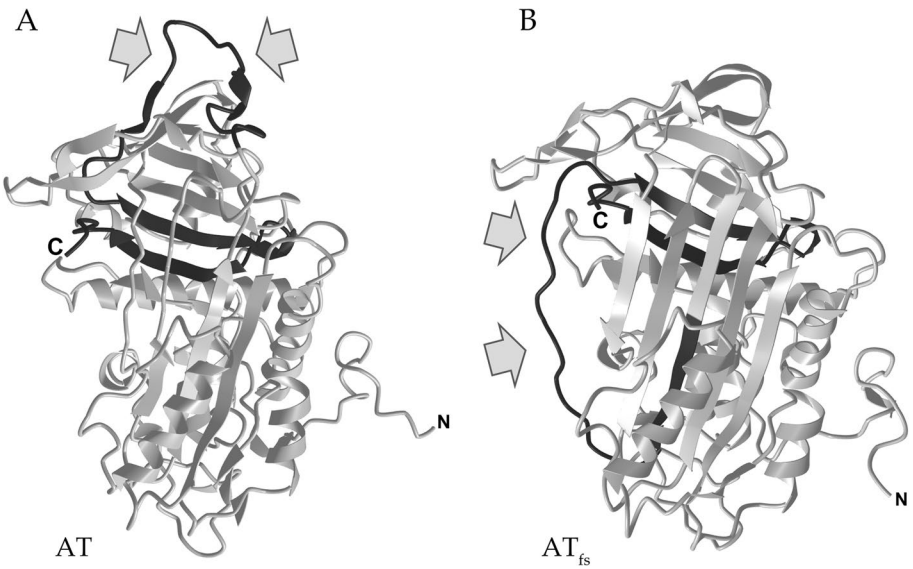

Fig. 4 Predicted tertiary structures for WT AT and p.Ser417LysfsTer48 variant (AT_{fs}). Native form of AT is indicated by the exposed reactive center loop (**A**, indicated by arrows). In silico prediction by C-I-TASSER [9] results in a folding model of AT_{fs} that resembles the latent form of SERPINs. The C-terminal peptide of AT_{fs} with altered amino acid sequence according to the frameshift mutation is differentially positioned in AT_{fs} (**B**, indicated by arrows)

Since the frameshift mutation also affects the reactive center loop, the peptide at the respective position in AT_{fs} is not exposed as in native AT [26] (indicated by gray arrows in Fig. 4A), but shifted into a position mimicking the latent form of SERPIN proteins [27] (gray arrows in Fig. 4B).

The latent form of SERPINS is usually described as unable to polymerize, as the annealing site of β-sheet A is occupied and thus not available for polymerization [28].

Here, it is important to point out that algorithm-based models are known to have their limitations, as they rely on (a) the availability of high-quality structural data and (b) should consequently only be used an approximation, with recent examples highlighting structural und functional protein differences between in silico predictions and in vitro evidence [29–31]. A recent publication confirms this for five *SERPINC1* mutations resulting in AT deficiency, with conformational structures obtained from experimental evidence significantly differing from the computational predictions [32]. Thus, a possibly different conformation of AT_{fs} and hence a polymerization cannot be ruled out.

Recognition of incorrectly folded proteins is based on the presence of processed N-glycans [33], exposed hydrophobic surfaces [34, 35] or free thiols [36–38]. Structural integrity of AT is provided by three disulfide bonds (Cys40-Cys160, Cys53-Cys127, Cys279-Cys462) [39], with the C-terminal disulfide bond Cys279-Cys462 being critical for initiating a proper folding [40]. Interestingly, although frameshift mutation p.Ser417LysfsTer48 affects Cys462, a Cys at almost similar position is given by default (AT_{fs}-Cys463; Fig. 1).

The predicted SERPIN-like structure of AT_{fs} may provide the necessary proximity of Cys40/Cys160, Cys53/Cys127 and Cys279/AT_{fs}-Cys463 for the formation of disulfide bonds. However, the mutated C-terminus of AT_{fs} contains further Cys residues (AT_{fs}-Cys420, AT_{fs}-Cys421 and AT_{fs}-Cys423; Fig. 1A). It was recently shown that the ER quality control for human AT exclusively relies on the thiol-dependent quality control [41]. A Cys-less AT mutant, which was shown to be misfolded and inactive, was nevertheless secreted via the conventional secretory pathway [41]. In contrast, AT variants with free thiol groups were retained in the ER [41]. Regardless of whether a potential C-terminal disulfide bond between Cys279 and AT_{fs}-Cys463 is formed, there are three additional free thiol groups in AT_{fs} that will put the attention of the thiol-dependent quality control onto AT_{fs}. This might explain why several other + 1 frameshift C-terminal AT variants (that do not possess additional Cys residues) are still properly secreted [14], but, in contrast, AT_{fs} is not. Failure in passing the thiol-dependent quality control might not only explain the defect in secretion, but would also be in line with the observed AT deficiency in our patients.

Thus, at least two possible mechanisms could be causative for the impaired secretion of AT_{fs} – polymerization due to aberrant folding or the presence of additional free thiol groups. Further research including conformational studies of AT_{fs} and the exchange of additional Cys residues in AT_{fs} against Ala will help to elucidate which molecular mechanism causes the secretion defect resulting in AT deficiency.

Secretion defects are often based on impaired protein folding, which leads to intervention of the ER quality control system and subsequent ER-associated protein degradation (ERAD) [34, 42–44]. The use of proteasome inhibitors emphasized the degradation of different AT mutants [45, 46] and other mutated proteins from the SERPIN family [47–51] via ERAD and might also elucidate the probably ERAD-dependent degradation of AT_{fs}.

AT deficiency and, moreover, combined defects such as AT deficiency and FVL, as reported in our patients, are a strong risk factor for thrombotic events. A meta-analysis of 19 studies reports an estimated odds ratio of 14.0 for venous thromboembolism in patients with AT deficiency [52] while another meta-analysis, summarizing eight studies, reports an odds ratio of 4.17 for FVL [53]. Comparably, the annual incidence for thrombosis is 1.7% for individuals with AT deficiency and 0.1–0.2% for patients with FVL (with 0.01% in the overall population without identified genetic predisposition) [5]. Moreover, patients with AT deficiency are younger on average (around 40 years) when their first thrombotic event occurs than those with a heterozygous FVL mutation (around 60 years) [54]. Therefore, since the AT deficiency is a strong risk factor and because the patients suffered their first thromboembolic event at a young age, it is more likely that the AT deficiency had greater impact on the thrombotic events in the patients.

Conclusion

Here, we describe for the first time mutation c.1247dupC (p.Ser417LysfsTer48) as causative in patients suffering from type I AT deficiency. A clear defect in secretion of the GFP- or HA-tagged AT_{fs} was shown in a HEK293T in vitro expression system. Impaired secretion of AT_{fs} might be caused by polymerization induced by aberrant folding or by new Cys residues introduced by the frameshift mutation, providing free thiol groups that are recognized by the thiol-dependent ER quality control.

Abbreviations

AT	Antithrombin
AT_{fs}	Antithrombin with p.Ser417LysfsTer48 mutation
CDS	Coding sequence
DVT	Deep vein thrombosis
ER	Endoplasmic Reticulum
ERAD	Endoplasmic Reticulum-associated protein degradation
FVL	Factor V Leiden
GFP	Green fluorescent protein
HA	Hemagglutinin
SERPIN	Serine protease inhibitor
SSP-PCR	Sequence specific primer-polymerase chain reaction

Supplementary Information

The online version contains supplementary material available at https://doi.org/10.1186/s12959-024-00589-5.

Additional file 1: Supplemental Figure 1. Screening of healthy donors 1-93 for WT allele. **Supplemental Figure 2.** Screening of healthy donors 1-93 for mutant allele. **Supplemental Figure 3.** Screening of healthy donors 94-186 for WT allele. **Supplemental Figure 4.** Screening of healthy donors 94-186 for mutant allele. **Supplemental Figure 5.** Screening of healthy donors 187-279 for WT allele. **Supplemental Figure 6.** Screening of healthy donors 187-279 for mutant allele. **Supplemental Figure 7.** Screening of healthy donors 280-360 for WT allele. **Supplemental Figure 8.** Screening of healthy donors 280-360 for mutant allele. **Supplemental Figure 9.** Repetition of PCRs with no or positive results in first PCR.

Acknowledgements

We thank all patients and donors for providing blood at the Clinical Department of Transfusion Medicine and Hemostaseology in Erlangen and all colleagues involved for supporting this study. The present work was performed in fulfillment of the requirements for obtaining the degree "Dr. med." for Maximilian Ruf.

Conflict of interest

The authors declare that they have no conflicts of interest.

Authors' contributions

HH, SC and SS designed the work. RB designed and supervised all cloning steps. MR, AW, SC and SS performed research and analyzed the data. MR and SS wrote the article. HH, SA, JS, RB and SC substantively revised the manuscript. All authors read and approved the final manuscript.

Funding

Open Access funding enabled and organized by Projekt DEAL. We acknowledge financial support by the Deutsche Forschungsgemeinschaft and Friedrich-Alexander-University Erlangen-Nürnberg (FAU) within the funding program "Open Access Publication Funding".

Availability of data and materials

The datasets used and analyzed during the current study are available from the corresponding author on reasonable request.

Declarations

Ethics approval and consent to participate

The study was conducted in accordance with the Declaration of Helsinki, and approved by the Ethics Committee of the Friedrich-Alexander-University Erlangen-Nürnberg (FAU). Informed written consent was obtained from both patients (ethics committee vote #477_ 20 B) and healthy blood donors (ethics committee vote #357_19 B, #343_18 B).

Consent for publication

Not applicable.

Competing interests

The authors declare no competing interests.

Received: 31 August 2023 Accepted: 1 February 2024
Published online: 12 February 2024

References

1. Lane DA, Caso R. Antithrombin: structure, genomic organization, function and inherited deficiency. Baillière's Clin Haematol. 1989;2:961–98.
2. Lane DA, Bayston T, Olds RJ, Fitches AC, Cooper DN, Millar DS, et al. Antithrombin mutation database: 2nd (1997) update. For the plasma coagulation inhibitors subcommittee of the scientific and standardization committee of the International Society on thrombosis and Haemostasis. Thromb Haemost. 1997;77:197–211.
3. Heit JA. Thrombophilia: clinical and laboratory assessment and management. In: Kitchens CS, Alving BM, Kessler CM, editors. Consultative hemostasis and thrombosis. 2nd ed. Philadelphia: W.B. Saunders; 2007. p. 211–44.
4. Freed J, Bauer KA. Thrombophilia: clinical and laboratory assessment and management. In: Kitchens CS, Kessler CM, Konkle BA, Streiff MB, Garcia DA, editors. Consultative hemostasis and thrombosis. 4th ed. Philadelphia: Elsevier; 2019. p. 242–65.
5. Merriman L, Greaves M. Testing for thrombophilia: an evidence-based approach. Postgrad Med J. 2006;82:699–704.
6. Schneider S, Reißig J, Weisbach V, Achenbach S, Strobel J, Hackstein H, Protein S. Erlangen: a novel *PROS1* gene mutation associated with quantitative protein S deficiency. Blood Coagul Fibrinolysis. 2022;33:224–7.
7. Gibson DG, Young L, Chuang RY, Venter JC, Hutchison CA III, Smith HO. Enzymatic assembly of DNA molecules up to several hundred kilobases. Nat Methods. 2009;6:343–5.
8. Zheng L, Baumann U, Reymond JL. An efficient one-step site-directed and site-saturation mutagenesis protocol. Nucleic Acids Res. 2004;32:e115–e115.
9. Zheng W, Zhang C, Li Y, Pearce R, Bell EW, Zhang Y. Folding non-homologous proteins by coupling deep-learning contact maps with I-TASSER assembly simulations. Cell Rep Methods. 2021;1:100014.
10. Wang J, Youkharibache P, Zhang D, Lanczycki CJ, Geer RC, Madej T, et al. iCn3D, a web-based 3D viewer for sharing 1D/2D/3D representations of biomolecular structures. Bioinformatics. 2020;1:131–5.
11. Wang J, Youkharibache P, Marchler-Bauer A, Lanczycki C, Zhang D, Lu S, et al. iCn3D: from web-based 3D viewer to structural analysis tool in batch mode. Front Mol Biosci. 2022;9: 831740.
12. Perry DJ, Daly M, Harper PL, Tait RC, Price J, Walker ID, et al. Antithrombin Cambridge II, 384 ala to ser further evidence of the role of the reactive centre loop in the inhibitory function of the serpins. FEBS Lett. 1991;285:248–50.
13. Molho-Sabatier P, Aiach M, Gaillard I, Fiessinger JN, Fischer AM, Chadeuf G, et al. Molecular characterization of antithrombin III (ATIII) variants using polymerase chain reaction. Identification of the ATIII Charleville as an Ala 384 Pro mutation. J Clin Investig. 1989;84:1236–42.
14. Bravo-Pérez C, Toderici M, Chambers JE, Martínez-Menárguez JA, Garrido-Rodriguez P, Pérez-Sanchez H, et al. Full-length antithrombin frameshift variant with aberrant C-terminus causes endoplasmic reticulum retention with a dominant-negative effect. JCI Insight. 2022;7:19.
15. Bravo-Pérez C, de la Morena-Barrio ME, de la Morena-Barrio B, Miñano A, Padilla J, Cifuentes R, et al. Molecular and clinical characterization of transient antithrombin deficiency: a new concept in congenital thrombophilia. Am J Hematol. 2022;97:216–25.
16. Mushunje A, Zhou A, Carrell RW, Huntington JA. Heparin-induced substrate behavior of antithrombin Cambridge II. Blood. 2003;102:4028–34.
17. Bruce D, Perry DJ, Borg JY, Carrell RW, Wardell MR. Thromboembolic disease due to thermolabile conformational changes of antithrombin Rouen-VI (187 Asn–> asp). J Clin Investig. 1994;94:2265–74.
18. Picard V, Dautzenberg MD, Villoutreix BO, Orliaguet G, Alhenc-Gelas M, Aiach M. Antithrombin Phe229Leu: a new homozygous variant leading to spontaneous antithrombin polymerization in vivo associated with severe childhood thrombosis. Blood. 2003;102:919–25.
19. Corral J, Huntington JA, Gonzalez-Conejero R, Mushunje A, Navarro M, Marco P, et al. Mutations in the shutter region of antithrombin result in

formation of disulfide-linked dimers and severe venous thrombosis. J Thromb Haemost. 2004;2:931–9.
20. Whisstock JC, Silverman GA, Bird PI, Bottomley SP, Kaiserman D, Luke CJ, et al. Serpins flex their muscle: II. Structural insights into target peptidase recognition, polymerization, and transport functions. J Biol Chem. 2010;285:24307–12.
21. Khan MS, Singh P, Azhar A, Naseem A, Rashid Q, Kabir MA, et al. Serpin inhibition mechanism: a delicate balance between native metastable state and polymerization. J Amino Acids. 2011;2011:606797.
22. Roussel BD, Irving JA, Ekeowa UI, Belorgey D, Haq I, Ordóñez A, et al. Unravelling the twists and turns of the serpinopathies. FEBS J. 2011;278:3859–67.
23. Iwaki T, Nagahashi K, Takano K, Suzuki-Inoue K, Kanayama N, Umemura K, et al. Mutation in a highly conserved glycine residue in strand 5B of plasminogen activator inhibitor 1 causes polymerisation. Thromb Haemost. 2017;117:860–9.
24. Jochmans K, Lissens W, Vervoort R, Peeters S, De Waele M, Liebaers I. Antithrombin-gly 424 arg: a novel point mutation responsible for type 1 antithrombin deficiency and neonatal thrombosis. Blood. 1994;83:146–51.
25. Davis RL, Shrimpton AE, Carrell RW, Lomas DA, Gerhard L, Baumann B, et al. Association between conformational mutations in neuroserpin and onset and severity of dementia. Lancet. 2002;359:2242–7.
26. Grover SP, Mackman N. Anticoagulant SERPINs: endogenous regulators of hemostasis and thrombosis. Front Cardiovasc Med. 2022;9: 878199.
27. Law RH, Zhang Q, McGowan S, Buckle AM, Silverman GA, Wong W, et al. An overview of the serpin superfamily. Genome Biol. 2006;7:1–11.
28. Onda M, Belorgey D, Sharp LK, Lomas DA. Latent S49P neuroserpin forms polymers in the dementia familial encephalopathy with neuroserpin inclusion bodies. J Biol Chem. 2005;280:13735–41.
29. Sanavia T, Birolo G, Montanucci L, Turina P, Capriotti E, Fariselli P. Limitations and challenges in protein stability prediction upon genome variations: towards future applications in precision medicine. Comput Struct Biotechnol J. 2020;18:1968–79.
30. Bertoline LM, Lima AN, Krieger JE, Teixeira SK. Before and after AlphaFold2: an overview of protein structure prediction. Front Bioinform. 2023;3:1120370.
31. Varadi M, Bordin N, Orengo C, Velankar S. The opportunities and challenges posed by the new generation of deep learning-based protein structure predictors. Curr Opin Struct Biol. 2023;79: 102543.
32. Garrido-Rodriguez P, Carmena-Bargueno M, de la Morena-Barrio ME, Bravo-Perez C, de la Morena-Barrio B, Cifuentes-Riquelme R, et al. Analysis of AlphaFold and molecular dynamics structure predictions of mutations in serpins. BioRxiv. 2023;2023–01.
33. Hebert DN, Molinari M. Flagging and docking: dual roles for N-glycans in protein quality control and cellular proteostasis. Trends Biochem Sci. 2012;37:404–10.
34. Ellgaard L, Helenius A. Quality control in the endoplasmic reticulum. Nat Rev Mol Cell Biol. 2003;4:181–91.
35. Kim YE, Hipp MS, Bracher A, Hayer-Hartl M, Hartl FU. Molecular chaperone functions in protein folding and proteostasis. Annu Rev Biochem. 2013;82:323–55.
36. Isidoro C, Maggioni C, Demoz M, Pizzagalli A, Fra AM, Sitia R. Exposed thiols confer localization in the endoplasmic reticulum by retention rather than retrieval. J Biol Chem. 1996;271:26138–42.
37. Wang ZV, Schraw TD, Kim J-Y, Khan T, Rajala MW, Follenzi A, et al. Secretion of the adipocyte-specific secretory protein adiponectin critically depends on thiol-mediated protein retention. Mol Cell Biol. 2007;27:3716–31.
38. Anelli T, Sannino S, Sitia R. Proteostasis and redoxtasis in the secretory pathway: tales of tails from ERp44 and immunoglobulins. Free Radic Biol Med. 2015;83:323–30.
39. van Boven HH, Lane DA. Antithrombin and its inherited deficiency states. Semin Hematol. 1997;34:188–204.
40. Chandrasekhar K, Ke H, Wang N, Goodwin T, Gierasch LM, Gershenson A, et al. Cellular folding pathway of a metastable serpin. PNAS. 2016;113:6484–9.
41. Adams BM, Ke H, Gierasch LM, Gershenson A, Hebert DN. Proper secretion of the serpin antithrombin relies strictly on thiol-dependent quality control. J Biol Chem. 2019;294:18992–9011.
42. Brodsky JL, McCracken AA. ER protein quality control and proteasome-mediated protein degradation. Sem Cell Dev Biol. 1999;10:507–13.
43. Meusser B, Hirsch C, Jarosch E, Sommer T. ERAD: the long road to destruction. Nat Cell Biol. 2005;7:766–72.
44. Needham PG, Guerriero CJ, Brodsky JL. Chaperoning endoplasmic reticulum–associated degradation (ERAD) and protein conformational diseases. Cold Spring Harb Perspec Biol. 2019;11:a033928.
45. Tokunaga F, Shirotani H, Hara K, Kozuki D, Omura S, Koide T. Intracellular degradation of secretion defect-type mutants of antithrombin is inhibited by proteasomal inhibitors. FEBS Lett. 1997;412:65–9.
46. Shirotani H, Tokunaga F, Koide T. Cellular and functional characterization of three recombinant antithrombin mutants that caused pleiotropic effect-type deficiency. J Biochem. 1999;125:253–62.
47. Qu D, Teckman JH, Omura S, Perlmutter DH. Degradation of a mutant secretory protein, α1-antitrypsin Z, in the endoplasmic reticulum requires proteasome activity. J Biol Chem. 1996;271:22791–5.
48. Teckman JH, Burrows J, Hidvegi T, Schmidt B, Hale PD, Perlmutter DH. The proteasome participates in degradation of mutant α1-antitrypsin Z in the endoplasmic reticulum of hepatoma-derived hepatocytes. J Biol Chem. 2001;276:44865–72.
49. Kroeger H, Miranda E, MacLeod I, Perez J, Crowther DC, Marciniak SJ, et al. Endoplasmic reticulum-associated degradation (ERAD) and autophagy cooperate to degrade polymerogenic mutant serpins. J Biol Chem. 2009;284:22793–802.
50. Christiansen HE, Schwarze U, Pyott SM, AlSwaid A, Al Balwi M, Alrasheed S, et al. Homozygosity for a missense mutation in SERPINH1, which encodes the collagen chaperone protein HSP47, results in severe recessive osteogenesis imperfecta. Am J Hum Genet. 2010;86:389–98.
51. Ying Z, Wang H, Fan H, Wang G. The endoplasmic reticulum (ER)-associated degradation system regulates aggregation and degradation of mutant neuroserpin. J Biol Chem. 2011;286:20835–44.
52. Croles FN, Borjas-Howard J, Nasserinejad K, Leebeek FW, Meijer K. Risk of venous thrombosis in antithrombin deficiency: a systematic review and bayesian meta-analysis. In: seminars in thrombosis and hemostasis. Thieme Med Publishers. 2018;44:315–26.
53. Castaman G, Faioni EM, Tosetto A, Bernardi F. The factor V HR2 haplotype and the risk of venous thrombosis: a meta-analysis. Haematologica. 2003;88:1182–9.
54. Vossen CY, Conard J, Fontcuberta J, Makris M, Van der Meer FJM, Pabinger I, et al. Risk of a first venous thrombotic event in carriers of a familial thrombophilic defect. The European prospective cohort on thrombophilia (EPCOT). J Thromb Haemost. 2005;3:459–64.

Publisher's Note